Fractional Entropy of Multichannel Kondo Systems from Conductance-Charge Relations

Cheolhee Han,[1] Z. Iftikhar,[2] Yaakov Kleeorin,[3] A. Anthore,[2,4] F. Pierre,[2] Yigal Meir,[5]
Andrew K. Mitchell[6,7,*] and Eran Sela[1,†]

[1]*Raymond and Beverly Sackler School of Physics and Astronomy, Tel Aviv University, Tel Aviv 69978, Israel*
[2]*Université Paris-Saclay, CNRS, Centre de Nanosciences et de Nanotechnologies (C2N), 91120 Palaiseau, France*
[3]*Center for the Physics of Evolving Systems, University of Chicago, Chicago, Illinois 60637, USA*
[4]*Université de Paris, F-75006 Paris, France*
[5]*Department of Physics, Ben-Gurion University of the Negev, Beer-Sheva 84105, Israel*
[6]*School of Physics, University College Dublin, Belfield, Dublin 4, Ireland*
[7]*Centre for Quantum Engineering, Science, and Technology, University College Dublin, Dublin 4, Ireland*

Fractional entropy is a signature of nonlocal degrees of freedom, such as Majorana zero modes or more exotic non-Abelian anyons. Although direct experimental measurements remain challenging, Maxwell relations provide an indirect route to the entropy through charge measurements. Here we consider multichannel charge-Kondo systems, which are predicted to host exotic quasiparticles due to a frustration of Kondo screening at low temperatures. In the absence of experimental data for the charge occupation, we derive relations connecting the latter to the conductance, for which experimental results have recently been obtained. Our analysis indicates that Majorana and Fibonacci anyon quasiparticles are well developed in existing two- and three-channel charge-Kondo devices, and that their characteristic $k_B \log \sqrt{2}$ and $k_B \log[(1 + \sqrt{5})/2]$ entropies are experimentally measurable.

A plethora of condensed-matter systems are conjectured to support exotic quasiparticles, which may serve as basic ingredients for quantum technologies [1]. However, the experimental demonstration is debated, and an unambiguous observation is still lacking. For example, current experimental evidence for the observation of Majorana fermions (MFs) is based on measurements of zero-bias peaks in the differential conductance which, however, may be attributable to other sources [2]. By contrast, thermodynamic quantities can unambiguously distinguish MFs from simpler excitations [3–5]. In particular, the additional entropy due to a single Majorana fermion is $S = \frac{1}{2} k_B \log 2$—half that of a regular spin-degenerate state. This fractional entropy implies that information is stored nonlocally across a pair of decoupled bound states. The measurement of a fractional entropy would therefore serve as a smoking-gun signature for exotic quasiparticles [6,7].

In the context of the low-dimensional mesoscopic electronic systems predicted to host exotic quasiparticles, thermodynamic quantities are unfortunately difficult to measure experimentally. Techniques developed to measure extensive properties in bulk systems are inapplicable to identify small changes due to individual excitations over the large background phonon contributions. Thus observation of fractional entropy remains elusive. Two indirect approaches to entropy measurement have been developed recently in nanoelectronic devices, although neither has as yet been applied to a system hosting exotic quasiparticles.

One method utilizes thermopower measurements [8], while the other exploits a Maxwell relation connecting entropy changes to *charge* measurements [7,9,10].

In this Letter we discuss the latter approach in the context of charge-Kondo quantum dot devices [11,12]. These experimental systems are highly accurate circuit realizations of multichannel Kondo (MCK) models [11–18]. Because of a frustration of Kondo screening at low temperatures, the two-channel charge-Kondo (2CK) model supports a Majorana fermion, with a residual "impurity" entropy $S_{2CK} = k_B \log \sqrt{2}$, while the three-channel (3CK) model hosts a Fibonacci anyon as manifested by a residual entropy $S_{3CK} = k_B \log \phi$, where $\phi = \frac{1}{2}(1 + \sqrt{5})$ is the golden ratio [14,19,20]. The central question we address in this work is the following: can these predicted MCK fractional entropies be measured and distinguished, taking into account the complexities and limitations of the experimental realization?

So far, only the electrical conductance of charge-Kondo devices has been measured experimentally [11,12,21], and so here we make use of this existing data by deriving novel exact relations between the conductance G and the temperature-dependence of the dot occupation, dN/dT. Such relations are bijective and universal when the underlying physics is governed by a single energy scale, such as the Kondo temperature. The entropy is then extracted via a Maxwell relation [9]. Assuming that the charge sensing protocol is minimally invasive, we conclude that the

experimental observation of a nontrivial temperature scaling toward the ideal fractional values of the 2CK and 3CK entropy is entirely feasible. The method can be generalized to other systems, although the relations themselves are model specific.

Multichannel Kondo models.— A single spin-$\frac{1}{2}$ "impurity" coupled antiferromagnetically to one or more independent conduction electron channels represents an important paradigm in the theory of strongly correlated electrons. At high temperatures, the impurity is effectively free, and so the impurity contribution to the total system entropy is $S_{\rm CB} = \log 2$ (setting $k_B \equiv 1$ here and in the following). The impurity becomes strongly entangled with conduction electrons in a surrounding "Kondo cloud" [22,23] at low temperatures $T \ll T_K$, where T_K is the Kondo temperature. In the single-channel case, the conduction electrons exactly screen the impurity spin by formation of a many-body Kondo singlet, leaving zero residual entropy, $S_{\rm 1CK} = 0$. For $k \geq 2$ channels, the frustration of Kondo screening results in an "overscreened" scenario [14,19,20] with a finite residual entropy $S_{k{\rm CK}} = \log\{2\cos[\pi/(2+k)]\}$, a hallmark of non-Fermi liquid (NFL) physics. In particular, the impurity in the 2CK model

hosts an effective Majorana fermion at low temperatures [24] with $S_{\rm 2CK} = \log\sqrt{2}$, while $S_{\rm 3CK} = \log\phi$, corresponding to a Fibonacci anyon, is predicted for 3CK [25,26].

Charge-Kondo realization.— The charge 2CK and 3CK effects were demonstrated [11,12] in a metallic quantum dot (QD) tunnel coupled via quantum point contacts (QPCs) to two or three leads, as illustrated in the inset to Fig. 1(b). The device is operated in a large magnetic field such that the QD and leads are in the quantum Hall regime, and the QPCs each consist of a pair of counterpropagating spinless fermions, one incoming into the QD and the other outgoing from the QD. The Hamiltonian of the k-channel charge-Kondo model reads as

$$H = \hbar v_F \sum_{j=1}^{k} \sum_{\nu={\rm in,out}} \int dx\, \psi_{j\nu}^{\dagger} i\partial_x \psi_{j\nu} + E_C(\hat{N} - N_g)^2$$

$$+ \hbar v_F \sum_{j=1}^{k} (r_j \psi_{j{\rm in}}^{\dagger}(0)\psi_{j{\rm out}}(0) + {\rm H.c.}). \quad (1)$$

The first term describes the free fermion modes $\psi_{j\nu}$ (with Fermi velocity v_F), while the second term describes the dot
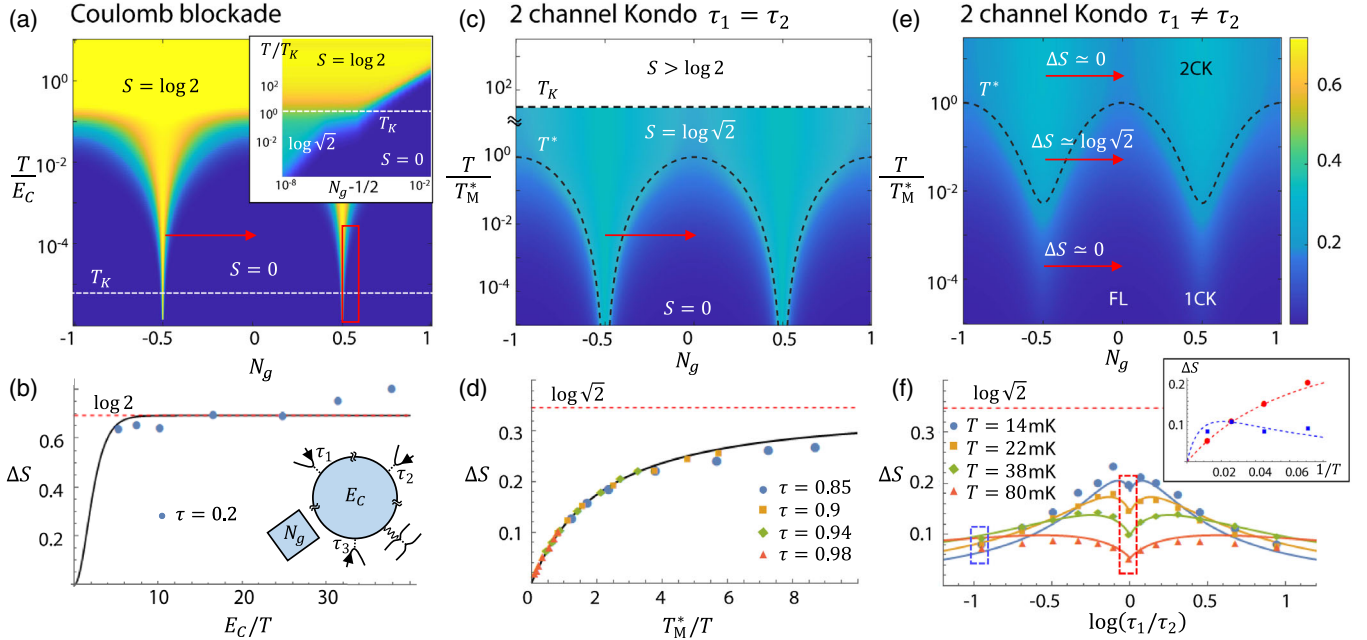

FIG. 1.   (a) Phase diagram of the charge k-channel Kondo device. For $T \gg T_K$ the entropy is $S = \log 2$ (yellow) at charge degeneracy $N_g = \pm\frac{1}{2}$, but $S = 0$ (blue) in the Coulomb valley when $T \ll E_C$. Inset: expanded view of red box, where the $k = 2$ system maps to the 2CK model and the entropy for $T \ll T_K$ (obtained by NRG) approaches $\log\sqrt{2}$. (b) Entropy difference along the red arrow in (a) obtained from experimental conductance data for $\tau = 0.2$ and $T/{\rm mK} = 7.9, 9.5, 12, 18, 28.9, 40$, and 55 via Eqs. (2) and (3) (points) compared with Eq. (4) (line). Inset: device schematic for $k = 3$. (c) 2CK phase diagram and impurity entropy, showing the NFL-FL crossover on the scale of T^* along the red arrow. (d) Entropy change extracted from the experimental 2CK conductance data via Eqs. (2) and (5) (points) as a function of T_M^*/T for different τ, compared with Eq. (6) (line). (e) Phase diagram of channel-asymmetric 2CK system with $\tau_1 \neq \tau_2$, showing finite T^* even at $N_g = \frac{1}{2}$. The low-T suppression of impurity entropy results in the nonmonotonic behavior of ΔS on decreasing T. (f) Extracted entropy from experimental data as for (d) but for $\tau_1 \neq \tau_2$, showing the NFL-FL crossover. For $\log(\tau_1/\tau_2) < 0 (> 0)$, we set $\tau_2 (\tau_1)$ to 0.93 and vary $\tau_1 (\tau_2)$. Inset: temperature dependence of ΔS for $\tau_1 = \tau_2$ (red) and $\tau_1 \neq \tau_2$ (blue) corresponding to the dashed boxes.

interactions with E_C the charging energy and $\hat{N}$ the electron number of the QD. N_g is the gate voltage applied to the dot, normalized such that $N_g = 1$ corresponds to the addition of a single electron to the dot. The last term describes the reflection amplitude r_j at each QPC, related to the transmission coefficient τ_j as $1 - \tau_j \simeq r_j^2$ [27,28].

The charge degeneracy at a Coulomb peak ($N_g = \frac{1}{2}$) maps to an effective impurity pseudospin-$\frac{1}{2}$ [17]; tunneling at the QPCs then corresponds to pseudospin flip processes. The 2CK and 3CK models were found to accurately describe the experimental QD device with two and three leads by detailed comparison with electrical transport measurements [11,12,17,18]. The thermoelectric response (as yet unmeasured in these systems) was predicted in Refs. [34,35].

At the frustrated critical point, $r_j \equiv r$ (hence $\tau_j \equiv \tau$). The Kondo temperature T_K is determined by the transmission; at a given temperature T, small τ implies $T \gg T_K$ (where $T_K \propto E_C e^{-\pi^2/\sqrt{4\tau}}$) and so the system is in the classical Coulomb blockade (CB) regime, while for larger τ such that $T \ll T_K$ [e.g., $T_K \propto E_C/(1-\tau)$ for 2CK [11,17]], the system exhibits the overscreened MCK effect. By detuning the gate voltage, a crossover is induced from the NFL point with fractional entropy, to a Fermi liquid (FL) state with quenched impurity entropy [15–18].

Maxwell relation.—We focus on the entropy change ΔS occurring as the gate voltage is swept from $N_g = 0$ to $\frac{1}{2}$, corresponding to the crossover from the FL-trivial state with zero entropy, to the critical point which has fractional entropy for $T \ll T_K$. From theory we therefore expect $\Delta S(T)$ to approach S_{2CK} or S_{3CK} for the two- and three-channel charge-Kondo devices as T/T_K is lowered. The Maxwell relation relates this change to the gate-voltage integral of dN/dT viz.,

$$\Delta S = 2E_C \int_0^{1/2} dN_g \frac{dN}{dT}. \quad (2)$$

Entropy and conductance-charge relation in CB.— The system is in the CB regime for large QPC reflections, such that $E_C \gg T \gg T_K$. The phase diagram in this regime is depicted in Fig. 1(a), where the red arrow denotes the line along which the entropy change is measured. Here we expect $\Delta S \simeq \log 2$ since $S_{imp} \simeq 0$ at the Coulomb valley, while for $N_g = \frac{1}{2}$ the impurity spin-$\frac{1}{2}$ remains largely unscreened.

In the CB regime, both the conductance and the number of electrons in the dot can be obtained by classical rate equations,

$$\frac{dN_{CB}}{dT} = \frac{1}{2T} \tanh \frac{E_C(N_g - \frac{1}{2})}{T} \frac{\frac{2E_C}{T}(N_g - \frac{1}{2})}{\sinh[\frac{2E_C}{T}(N_g - \frac{1}{2})]}$$

$$\equiv \frac{1}{2T} \tanh \frac{E_C(N_g - \frac{1}{2})}{T} \frac{G_{CB}}{G_{CB,max}}, \quad (3)$$

where G_{CB} is the CB conductance and $G_{CB,max}$ is the Coulomb peak conductance (itself a function of τ and T [11,17]). Physically, this relation follows from the fact that both observables are proportional to the dot density of states. In deriving Eq. (3) we assumed $T \ll E_C$ and retained only two dot charge states (therefore it is not periodic in N_g and should be used only in the vicinity of a well-isolated CB peak). Within the same approximation, we can calculate the thermodynamic free energy and hence obtain a prediction for ΔS directly,

$$\Delta S_{CB} = \log 2 + \frac{E_C/T}{1 + e^{-E_C/T}} - \log(1 + e^{E_C/T}). \quad (4)$$

This result also coincides with that obtained from Eq. (2) using dN_{CB}/dT. Note that $\Delta S_{CB} \to \log 2$ as $T \to 0$, corresponding to the unscreened twofold charge degeneracy of the dot in the CB regime.

We now utilize experimental data for the CB conductance [11] and Eqs. (2) and (3) to obtain an estimate for ΔS_{CB} in the experimental setting of the charge-Kondo device. The results are plotted in Fig. 1(b), comparing with Eq. (4) (line). The agreement is good at higher temperatures as expected, although experimental noise around the low-conductance signal in the CB regime naturally introduces errors. At lower temperatures, deviations due to Kondo renormalization are observed. To capture the behavior in the Kondo regime, one must use a more sophisticated theory to obtain the full conductance-charge relation. While the theoretical curve displays a decay of ΔS_{CB} to zero for temperatures exceeding the charging energy, the present experimental data are restricted to temperatures up to 55 mK which is well below E_C. In the following we do this analytically for 2CK and numerically for 3CK.

Entropy and conductance-charge relation for 2CK.— We consider now the 2CK case with $\tau_1 = \tau_2 \equiv \tau$ and $T \ll T_K$ (large τ regime). A new energy scale is generated by gate-voltage detuning, $T^* = T_M^* \cos^2(\pi N_g)$, with $T_M^* = 8e^{\mathbf{C}} E_C(1-\tau)/\pi^2$ (and $\mathbf{C}$ the Euler constant). The NFL phase is stabilized for $T^* \ll T \ll T_K$, while for $T \ll T^*$ the system is in the zero-entropy, FL state—see Fig. 1(c). Thus, a fractional entropy change is expected along the red arrow, corresponding to the crossover between FL and NFL states. The model can be mapped to a resonant Majorana tunneling model [17,24,28]; this analytic solution allows us to obtain dN/dT as well as the relation between dN/dT and G at large τ:

$$\frac{dN_{2CK}}{dT} = \frac{T_M^* \sin(2\pi N_g)}{4E_C T} \left(1 - \frac{T^*}{2\pi T} \psi^{(1)} \left[\frac{1}{2} + \frac{T^*}{2\pi T}\right]\right)$$

$$\equiv \frac{T_M^* \sin(2\pi N_g)}{4E_C T} \frac{2G_{2CK}h}{e^2}. \quad (5)$$

For comparison, a direct calculation of the entropy yields

$$\Delta S_{2CK} = \frac{T_M^*[\psi(\frac{1}{2} + \frac{T_M^*}{2\pi T}) - 1]}{2\pi T} - \log\left[\frac{\Gamma(\frac{1}{2} + \frac{T_M^*}{2\pi T})}{\sqrt{\pi}}\right], \quad (6)$$

where $\psi(x)$ and $\psi^{(1)}(x)$ are the di-γ and tri-γ function, respectively.

We again use experimental conductance data [11] to obtain dN/dT via Eq. (5), taking the experimental values of E_C and τ—but now in the nontrivial Kondo regime of the two-lead device. The entropy change is then extracted from Eq. (2), and plotted in Fig. 1(d) for various values of τ. The experimental data are seen to collapse accurately onto the predicted scaling form of Eq. (6) (solid line) for large τ where the above relation applies, with the entropy change tending to $\Delta S \to S_{2CK}$ as the temperature is lowered. Appreciable deviations appear only for $\tau \lesssim 0.85$, for which the leading irrelevant operator must be taken into account in the theory [17,36].

We note that the impurity entropy at $N_g = 0$ does not reach zero even at the experimental base temperature of $T = 7.9$ mK for $E_C = 300$ mK, as reported in Ref. [11]. Therefore the measured entropy change is about 80% of the ideal 2CK bound $S_{2CK} = \log\sqrt{2}$. Our results (in particular the temperature scaling) are consistent with the formation of a single Majorana fermion on the dot, but the bound would be better saturated for larger E_C/T.

Next we consider the channel-asymmetric case where $\tau_1 \neq \tau_2$. On reducing the temperature, the system now flows from the 2CK critical point to a 1CK FL state with the more strongly coupled channel—see Fig. 1(e). Extending the theory to this case, the crossover scale marked as a dashed line in Fig. 1(e) becomes

$$T^* = \frac{2}{\pi^2}e^C E_C[2 - \tau_1 - \tau_2 + 2\sqrt{(1-\tau_1)(1-\tau_2)}\cos(4\pi N_g)]. \quad (7)$$

The relation between dN/dT and the conductance in Eq. (5) still holds once $(1 - \tau)$ in the expression for T_M^* is replaced by $\sqrt{(1 - \tau_1)(1 - \tau_2)}$. This shows how the fractional entropy in the NFL phase is quenched to zero as the channel asymmetry drives the system to the 1CK FL regime. Applying this relation to the available experimental conductance data [11] we obtain ΔS along this crossover. The entropy ΔS extracted in this way is in quantitative agreement with the direct calculation of the entropy, shown as solid lines in Fig. 1(f). Interestingly, ΔS is not a monotonic function of $\log(\tau_1/\tau_2)$. This is due to the fact that as one, e.g., decreases τ_2, T^* increases. As a consequence, the system is first driven closer to the 2CK fixed point, before turning over and flowing toward the 1CK fixed point. Similarly, ΔS is not a monotonic function of T; see Fig. 1(e) and the inset to Fig. 1(f).

Entropy and conductance-charge relation for 3CK.—We now turn to the critical 3CK system obtained by tuning

$\tau_1 = \tau_2 = \tau_3 \equiv \tau$ in the three-lead charge-Kondo device [12]. Here the situation is more complex theoretically, as an analytical solution along the NFL to FL crossover is not known. Instead we employ a numerical solution using state-of-the-art numerical renormalization group (NRG) calculations [37–39] to obtain the conductance G as well as dN/dT along the crossover.

By comparison of the NRG model predictions to the conductance data [12] we note that the experiment at large τ is not in the fully universal regime. In order to make our comparison with experiment quantitative, we generalize the standard 3CK model by retaining multiple dot charge states [28]. For each experimental conductance curve we fit the model parameters to best match the conductance line shapes. We consider a single (base) temperature of $T = 7.9$ mK, and transmissions ranging from $\tau = 0.79$ to $\tau = 0.198$ as in the experiment, which corresponds to the crossover regime from $T \ll T_K$ to $T \gg T_K$.

Figure 2(a) depicts the remarkable agreement between the experimental conductance curves and the NRG line shapes over the entire range of N_g for all values of the transmission considered. This again validates the theoretical model as an accurate description of the physical device. For these same parameters, NRG also yields dN/dT, and hence we deduce numerically the relation between G and dN/dT, as shown in Fig. 2(b). Unlike the CB and 2CK cases [Eqs. (3) and (5)], in 3CK, there is no simple relation between dN/dT and G [28]. Accordingly, for each set of
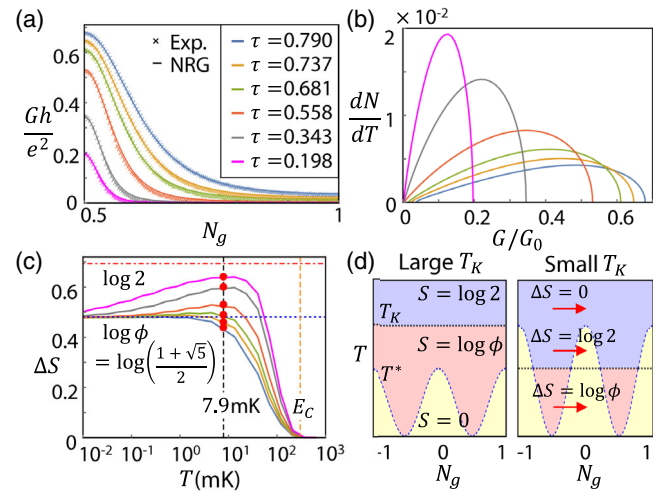

FIG. 2. (a) Conductance G for the 3CK system as a function of N_g for different τ at $T = 7.9$ mK, comparing experimental data (points) with NRG calculations (lines). (b) Numerically determined relation between dN/dT and G for the same model parameters as in (a). (c) 3CK entropy difference ΔS (points) from Eq. (2) using G from panel (a) and $dN/dT = f(G)$ from panel (b), compared with thermodynamic NRG results (lines). (d) Schematic phase diagrams for large transmission (left) and small transmission (right): CB regime in blue ($T \gg T_K$, $S = \log 2$), FL in yellow ($T \ll T^*$, $S = 0$), NFL in red ($T^* < T < T_K$, $S_{3CK} = \log\phi$).

parameters, we use the numerically obtained relation between dN/dT and G to determine the entropy difference ΔS via Eq. (2). These are marked as the circle points in Fig. 2(c).

The results are consistent with the entropy obtained from standard thermodynamic NRG calculations [Fig. 2(c), lines], which include the full temperature dependence. For larger transmissions we find a direct crossover from $\Delta S = 0$ to $\log \phi$ for $T \ll T_K$, corresponding to the 3CK NFL state hosting a Fibonacci anyon. Interestingly, for small τ we find that ΔS first approaches $\log 2$ for $T \gg T_K$ before approaching $\log \phi$ at the low-temperature limit. These two behaviors for large and small transmissions are illustrated in the two phase diagrams in Fig. 2(d). For large τ, due to large charge fluctuations, the 3CK Kondo temperature T_K well exceeds the N_g dependent crossover scale T^*. As a result, ΔS—which probes gate-voltage sensitivity—increases from 0 to $\log \phi$ as T is lowered below the crossover temperature T^*. For small transmissions, however, there are effectively only two accessible charge states, as in the familiar spin Kondo problem. Then we have a large gate-voltage sensitivity, which acts as an effective magnetic field on the impurity pseudospin. Similar to the situation shown in Fig. 1(a), above T_K the system is described by the CB theory, and below T_K there is a FL–NFL crossover, leading to the nonmonotonic behavior observed in Fig. 2(c) at small τ.

Conclusion.— Nanoelectronic devices offer a controllable route to realizing anyonic quasiparticles. Their existence can be demonstrated through their fractional entropy. Here we develop an indirect route to the latter in 2CK and 3CK systems by (i) exploiting a Maxwell relation connecting the entropy change ΔS to the charge variation dN/dT, and (ii) deriving relations between dN/dT and the measured electrical conductance G. Applying our methodology to existing conductance data for 2CK and 3CK charge-Kondo devices [11,12], we observe a scaling toward the expected nontrivial entropy value $S_{2CK} = \log \sqrt{2}$ for a Majorana anyon case. Likewise our analysis of the 3CK model for various transmission values is consistent with $S_{3CK} = \log \phi$ for a Fibonacci anyon. Although experimental charge measurements on these systems are required for the incontrovertible demonstration of fractional quasiparticles, our analysis shows that existing experiments do operate in the necessary regime, and that the protocol for the observation of fractional entropy via the Maxwell relation is feasible. Entropy spectroscopy could serve as a smoking-gun probe of exotic anyons in other more controversial systems such as Majorana wires [7,40] or other experimental systems realizing Kondo criticality [21,41–44].

*andrew.mitchell@ucd.ie
†eranst@post.tau.ac.il

[1] C. Nayak, S. H. Simon, A. Stern, M. Freedman, and S. Das Sarma, Non-abelian anyons and topological quantum computation, Rev. Mod. Phys. **80**, 1083 (2008).

[2] H. Pan and S. Das Sarma, Physical mechanisms for zerobias conductance peaks in majorana nanowires, Phys. Rev. Research **2**, 013377 (2020).

[3] N. R. Cooper and A. Stern, Observable Bulk Signatures of Non-Abelian Quantum Hall States, Phys. Rev. Lett. **102**, 176807 (2009).

[4] G. Viola, S. Das, E. Grosfeld, and A. Stern, Thermoelectric Probe for Neutral Edge Modes in the Fractional Quantum Hall Regime, Phys. Rev. Lett. **109**, 146801 (2012).

[5] G. Ben-Shach, C. R. Laumann, I. Neder, A. Yacoby, and B. I. Halperin, Detecting Non-Abelian Anyons by Charging Spectroscopy, Phys. Rev. Lett. **110**, 106805 (2013).

[6] K. Yang and B. I. Halperin, Thermopower as a possible probe of non-Abelian quasiparticle statistics in fractional quantum hall liquids, Phys. Rev. B **79**, 115317 (2009).

[7] E. Sela, Y. Oreg, S. Plugge, N. Hartman, S. Lüscher, and J. Folk, Detecting the Universal Fractional Entropy of Majorana Zero Modes, Phys. Rev. Lett. **123**, 147702 (2019).

[8] Y. Kleeorin, H. Thierschmann, H. Buhmann, A. Georges, L. W. Molenkamp, and Y. Meir, How to measure the entropy of a mesoscopic system via thermoelectric transport, Nat. Commun. **10**, 5801 (2019).

[9] N. Hartman, C. Olsen, S. Lüscher, M. Samani, S. Fallahi, G. C. Gardner, M. Manfra, and J. Folk, Direct entropy measurement in a mesoscopic quantum system, Nat. Phys. **14**, 1083 (2018).

[10] T. Child, O. Sheekey, S. Lüscher, S. Fallahi, G. C. Gardner, M. Manfra, Y. Kleeorin, Y. Meir, and J. Folk, Entropy measurement of a strongly correlated quantum dot, arXiv:2110.14158.

[11] Z. Iftikhar, S. Jezouin, A. Anthore, U. Gennser, F. Parmentier, A. Cavanna, and F. Pierre, Two-channel Kondo effect and renormalization flow with macroscopic quantum charge states, Nature (London) **526**, 233 (2015).

[12] Z. Iftikhar, A. Anthore, A. Mitchell, F. Parmentier, U. Gennser, A. Ouerghi, A. Cavanna, C. Mora, P. Simon, and F. Pierre, Tunable quantum criticality and super-ballistic transport in a "charge" Kondo circuit, Science **360**, 1315 (2018).

[13] P. Nozières and A. Bladin, Kondo effect in real metals, J. Phys. (Paris) **41**, 193 (1980).

[14] I. Affleck and A. W. W. Ludwig, Universal Noninteger "Ground-State Degeneracy" in Critical Quantum Systems, Phys. Rev. Lett. **67**, 161 (1991).

[15] K. A. Matveev, Quantum fluctuations of the charge of a metal particle under the coulomb blockade conditions, Sov. Phys. JETP **72**, 892 (1991).

[16] K. A. Matveev, Coulomb blockade at almost perfect transmission, Phys. Rev. B **51**, 1743 (1995).

[17] A. Furusaki and K. A. Matveev, Theory of strong inelastic cotunneling, Phys. Rev. B **52**, 16676 (1995).

[18] A. K. Mitchell, L. A. Landau, L. Fritz, and E. Sela, Universality and Scaling in a Charge Two-Channel Kondo Device, Phys. Rev. Lett. **116**, 157202 (2016).

[19] N. Andrei, Diagonalization of the Kondo Hamiltonian, Phys. Rev. Lett. **45**, 379 (1980).

[20] P. Wiegman, Exact solution of sd exchange model at $T = 0$, JETP Lett. **31**, 364 (1980).

[21] W. Pouse, L. Peeters, C. L. Hsueh, U. Gennser, A. Cavanna, M. A. Kastner, A. K. Mitchell, and D. Goldhaber-Gordon, Quantum simulation of an exotic quantum critical point in a two-site charge Kondo circuit, arXiv:2108.12691.

[22] A. K. Mitchell, M. Becker, and R. Bulla, Real-space renormalization group flow in quantum impurity systems: Local moment formation and the Kondo screening cloud, Phys. Rev. B **84**, 115120 (2011).

[23] I. V. Borzenets, J. Shim, J. C. H. Chen, A. Ludwig, A. D. Wieck, S. Tarucha, H.-S. Sim, and M. Yamamoto, Observation of the Kondo screening cloud, Nature (London) **579**, 210 (2020).

[24] V. J. Emery and S. Kivelson, Mapping of the two-channel Kondo problem to a resonant-level model, Phys. Rev. B **46**, 10812 (1992).

[25] P. L. S. Lopes, I. Affleck, and E. Sela, Anyons in multi-channel Kondo systems, Phys. Rev. B **101**, 085141 (2020).

[26] Y. Komijani, Isolating Kondo anyons for topological quantum computation, Phys. Rev. B **101**, 235131 (2020).

[27] C. de C. Chamon, D. E. Freed, S. A. Kivelson, S. L. Sondhi, and X. G. Wen, Two point-contact interferometer for quantum hall systems, Phys. Rev. B **55**, 2331 (1997).

[28] See Supplemental Material at http://link.aps.org/supplemental/10.1103/PhysRevLett.128.146803 for further details, which includes Refs. [29–33].

[29] K. Le Hur and G. Seelig, Capacitance of a quantudm dot from the channel-anisotropic two-channel Kondo model, Phys. Rev. B **65**, 165338 (2002).

[30] L. Glazman and M. Pustilnik, Coulomb blockade and Kondo effect in quantum dots, in *New Directions in Mesoscopic Physics (Towards Nanoscience)* (Springer, New York, 2003), pp. 93–115.

[31] A. Rozhkov, Impurity entropy for the two-channel Kondo model, Int. J. Mod. Phys. B **12**, 3457 (1998).

[32] E. L. Minarelli and A. K. Mitchell (to be published).

[33] J. B. Rigo and A. K. Mitchell, Automatic differentiable numerical renormalization group, Phys. Rev. Res. **4**, 013227 (2022).

[34] G. A. R. van Dalum, A. K. Mitchell, and L. Fritz, Wiedemann-Franz law in a non-Fermi liquid and Majorana central charge: Thermoelectric transport in a two-channel Kondo system, Phys. Rev. B **102**, 041111(R) (2020); Electric and heat transport in a charge two-channel Kondo device, Phys. Rev. B **102**, 205137 (2020).

[35] T. K. T. Nguyen and M. N. Kiselev, Thermoelectric Transport in a Three-Channel Charge Kondo Circuit, Phys. Rev. Lett. **125**, 026801 (2020).

[36] I. Affleck and A. W. Ludwig, Critical theory of overscreened Kondo fixed points, Nucl. Phys. **B360**, 641 (1991).

[37] K. G. Wilson, The renormalization group: Critical phenomena and the Kondo problem, Rev. Mod. Phys. **47**, 773 (1975); R. Bulla, T. A. Costi, and T. Pruschke, Numerical renormalization group method for quantum impurity systems, Rev. Mod. Phys. **80**, 395 (2008).

[38] A. Weichselbaum and J. von Delft, Sum-Rule Conserving Spectral Functions from the Numerical Renormalization Group, Phys. Rev. Lett. **99**, 076402 (2007).

[39] A. K. Mitchell, M. R. Galpin, S. Wilson-Fletcher, D. E. Logan, and R. Bulla, Generalized wilson chain for solving multichannel quantum impurity problems, Phys. Rev. B **89**, 121105(R) (2014).K. M. Stadler, A. K. Mitchell, J. von Delft, and A. Weichselbaum, Interleaved numerical renormalization group as an efficient multiband impurity solver, Phys. Rev. B **93**, 235101 (2016).

[40] S. Smirnov, Majorana tunneling entropy, Phys. Rev. B **92**, 195312 (2015).

[41] R. Potok, I. Rau, H. Shtrikman, Y. Oreg, and D. Goldhaber-Gordon, Observation of the two-channel Kondo effect, Nature (London) **446**, 167 (2007).

[42] A. Keller, L. Peeters, C. Moca, I. Weymann, D. Mahalu, V. Umansky, G. Zaránd, and D. Goldhaber-Gordon, Universal fermi liquid crossover and quantum criticality in a mesoscopic system, Nature (London) **526**, 237 (2015).

[43] A. K. Mitchell, A. Liberman, E. Sela, and I. Affleck, So (5) Non-Fermi Liquid in a Coulomb Box Device, Phys. Rev. Lett. **126**, 147702 (2021); A. Liberman, A. K. Mitchell, I. Affleck, and E. Sela, So (5) critical point in a spin-flavor Kondo device: Bosonization and refermionization solution, Phys. Rev. B **103**, 195131 (2021).

[44] H. Mebrahtu, I. Borzenets, H. Zheng, Y. V. Bomze, A. Smirnov, S. Florens, H. Baranger, and G. Finkelstein, Observation of majorana quantum critical behaviour in a resonant level coupled to a dissipative environment, Nat. Phys. **9**, 732 (2013).